An insight into the errors and uncertainty of the lithium-ion battery characterisation experiments

James Taylor[1], Anup Barai[1,*], T.R. Ashwin[1], Yue Guo[1], Mark Amor-Segan[1], James Marco[1]

[1]Energy Innovation Centre (EIC), WMG, University of Warwick, Coventry, CV4 7AL, United Kingdom

[*]Corresponding Author: a.barai@warwick.ac.uk

Highlights

- Errors need to be incorporated or at least their long-term implications understood
- A rigorous analysis of source of error in battery testing results presented
- Environmental errors can be identified and treated beforehand
- Careful evaluation of process and test data is required for procedural error
- Understanding sources of errors can result in significant improvements

Keywords

Battery testing; experimental error; standard error; test setup

Abstract

Errors and uncertainty within the experimental results have long-term implications in lithium-ion battery research. Experimental directly feed into the development of different battery models, thus having a direct impact on the accuracy of the models, which are commonly employed to forecast short to long term battery performance. The estimations made by such models underpin the design of key functions within the BMS, such as state of charge and state of health estimation. Therefore, erroneous experimental results could evolve into a much larger issue such as the early retirement of a battery pack from the end-use application. For original equipment manufacturers (OEM), such as automotive OEMs this may have a significant impact, e.g. high warranty returns and damage to the brand. Although occasionally reported in published results, currently, little research exists within the literature to systematically define the error and uncertainty of battery experimental results. This article focuses on the fundamental sources of error and uncertainty from experimental setup and procedure and suggests control measures to remove or minimize the contributions from the sources identified. Our research shows that by implementing the control measures proposed, the error and uncertainty can be reduced to around 0.6%, from the figure of around 4.0%.

1. Introduction

In tandem with the increasing demand of lithium-ion (li-ion) battery [1], the requirement of li-ion battery testing and characterisation has seen a significant rise in recent years. This increased demand for accurate and reliable testing and characterisation is derived from the requirement of original equipment manufacturers (OEM). In order to find an optimal li-ion battery for an application, OEMs utilize different battery models, e.g. electrochemical models [2-4], equivalent circuit models [5, 6], degradation models [7, 8]. These battery models also underpin the design of the key functions within the battery management system (BMS) control functions such as the, such as state of charge (SoC) and state of health (SoH) estimation and the design if the thermal management system (TMS). To facilitate the development of these battery models and estimation of the performance of candidate li-ion batteries, OEMs will perform a variety of different experiments.

Different national and international li-ion battery test standards currently exist to guide battery testing. However, researchers and engineers often go beyond the standards and develop their own tests that are aligned with their application. A recent review of battery testing and characterisation procedures has identified a collection of battery tests commonly employed, their advantages and disadvantages [9]. This study may lead to concise use and standardisation of future tests, which is not the focus of this manuscript, therefore, the readers interested are directed to that article. However, [9] raises concerns on the accuracy and reproducibility of the test data. The accuracy and reproducibility of the data generated plays a vital role when defining the accuracy of prediction of the models and thus the poor estimation of battery performance.

Within all research, ensuring experiments give accurate, repeatable, reproducible results should be a primary concern when designing the experiment. As a field highly dependent on experimental results, the extensive test programmes carried out as part of the on-going research into battery technologies is no different. Due to the diversity of the interest, such as long-term performance, degradation and second-life applications, the experiments undertaken are often several years long and resource intensive [10, 11], therefore, extra care needs to be given to the experimental design to maximise accuracy.

In li-ion cell experimentation, there are many variable factors, some controllable, others not, that can influence measurement accuracy. For example, room temperature and cell surface temperature can be controlled when a discharge capacity test is performed at different current rates. However, internal heat generation and thus internal temperature cannot be directly

controlled [12]. Moreover, the internal temperature and the propagation of heat to the cell surface depends on the thermal conductivity of the cell which is linked with the chemical composition and design of each battery. This measurement discrepancy can vary with the design of the cell format (e.g. pouch or cylindrical) and the total cell surface area (heat transfer area) exposed to ambient. Therefore, the uncertainty analysis reporting is of critical importance.

Although of critical importance, limited research currently exist within the literature. While most of the published literature reporting experimental results includes a summary of the expected errors within the results, a systematic approach to categorize and minimize them is currently not present.

In li-ion battery experiments the sources of error can be broadly categorised into two types: environmental errors and procedural errors. Environmental errors are those sources of error that are systematic to multiple experiments and can be controlled to a limited degree within known bounds. Environmental errors include ambient temperature and humidity conditions, equipment accuracy and resolution, manufacturing tolerances on battery samples and equipment used. An example can be found in [13], where similar tests (e.g. calendar life test at 80 % SoC at 40, 50, 60 and 70 °C) were performed in different laboratory on same type of cells, and 5-7 % error in data was reported, of which a large proportion may be environmental error. While steps can be taken to account for and control these sources, the error they contribute cannot be reduced without major changes to the experimental design, such as wholesale changes to experimental location and equipment. These errors, are however, consistent and can be documented when developing an experiment or analysing the results.

Procedural errors are the errors introduced as a result of performing the experiment. These types of error occur during the experimental process itself and are known to be more variable. Procedure errors include tester variation, set-up variation, sample variation, repeatability. Such errors are difficult to document in advance, and rely on performing the experiment itself in order to determine them. One example of such error can be found in [14, 15], where it was shown how battery's impedance varies after a charge/discharge event, if an adequate amount of relaxation period is not applied in the experimental procedure, the results will be erroneous. Once observed, unsatisfactory error levels can have actions taken against them in order to improve the quality of the results obtained, such as improved staff training, alterations to procedure or improved calibration of experimental elements.

The reporting of errors increases confidence in the experimental procedure and the data that has been produced. A quantitative measure of error established a priori to experimentation will help to improve the quality of the data produced by the experimentation and allow a researcher to ensure that experiments are being run at a suitable standard. Experimental errors are commonly reported via two models, experimental error and standard error.

Experimental error represents the combined contribution of all error effects, environmental and procedural, and gives information about the uncertainty of a particular experiment and the expected results from further repetition under similar conditions. Expressing an uncertainty interval means either: the reported result is a true representation, or the true results exist within the uncertainty region reported [16]. While useful for providing an indication of the quality of the result, it is difficult to interpret in a broader sense; for example, how does this error compare to dissimilar experiments or what can be done to improve the experimental accuracy and reproducibility.

Standard error is an alternative approach to reporting error, providing information on the second type of uncertainty. Standard error analyses the error contribution of elements to an experiment and determines the quality of the estimate [17]. Rather than illustrating where *results* are expected to fall, standard error defines where the *true* value is expected to be. With sufficient data acquired before experimentation, the standard error can be calculated in advance of performing an experiment and give an experimenter a quantitative measure of the quality of their results. For singular laboratory experiments, this level of analysis is more expensive to undertake than the experiment itself, but in a larger testing environment performing many similar experiments as part of a systematic test program, this approach becomes more valuable. This allows a research laboratory to report both their variance in results (experimental error) and the accuracy of their results (standard error) with more confidence.

Having these two types of error in agreement is the ideal result for an experiment, as this highlights that variability is minimised to its lowest achievable level. The standard error can be used to find possible areas of experimental improvement. In practice, the standard error will typically be less than the experimental error, as it is impossible to be certain that every possible source of error is included into the calculation of standard error, but a similar magnitude of uncertainty values still indicates the acceptable performance of the experiment.

The systematic nature of environmental errors allows them to be accounted for in the standard error model. Climatic control, measurement equipment accuracy and manufacturing tolerances

all contribute to standard error, and can often be obtained from supplier information or initial experimental results. Repeating measurements on a sample environment quickly collaborates such information, and ongoing data collection can be used to check calibration and continued accuracy levels. within a testing facility, such data should be readily available and employed to maintain levels of standard error for use in the design of experiments.

While experiments are varied and diverse in their research aims and goals, the procedures followed to perform experimental design contain a number of common elements such as equipment and personnel. These common elements are further increased through standardisation of approaches to improve efficiency and consistency of generated results. These experimental elements introduce error to the testing procedure, but can be studied employing benchmark testing and the errors introduced are quantified. This can be then used as a point to suggest improvements and repeat tests to accurately assess the impact on test error, leading to better procedures throughout the test facility. This reduces procedural errors and thus an overall improvement in reported experimental errors from experiments.

As part of this research, the testing procedures that define experiments were studied, both in text and in observation of the testing environment and practical application, with the aim to identify and quantify the main sources of environmental and procedural error that would produce uncertainty in measurements and quantify their impact on experimental results. While the broader research is being performed to capture all sources of error, however due to the limitation of the context of this article only three key sources are reported here.

This article will also present an example of how the reduction of errors within experimental data can directly feed into the development of empirical or semi-empirical models to improve the accuracy of the model estimation. The model estimation is directly employed to control the operating characteristics of the battery pack through the functions of the BMS. An erroneous experimentation, therefore, can result in erroneous controls and damage the battery before warranty period [18].

2. Experimental details

In light of the identified sources of environmental and procedural errors and their possible impact on test results, a series of experiments were devised to assess the procedure and to highlight further improvements.

2.1 Experiment 1 – researcher variation

The first test to be undertaken was to vary the researchers themselves. It is important that data be reproducible by other testers, and so the results need to be shown to be independent of the researcher carrying out the test. By establishing this, additional tests on the equipment and procedure can be undertaken with confidence in the reproducibility of the procedure when carried out by appropriately trained researchers.

Four researchers were selected to perform a pulse-power test (PPT) as outlined in IEC 62660-1 standard [19]. Testers performed PPT on 8 20 Ah cells. The pulses were 10 sec long with an amplitude outlined in Figure 1. The internal resistance was calculated form the voltage drop due to application of the pulse current. Further details on the procedure can be found in [20].

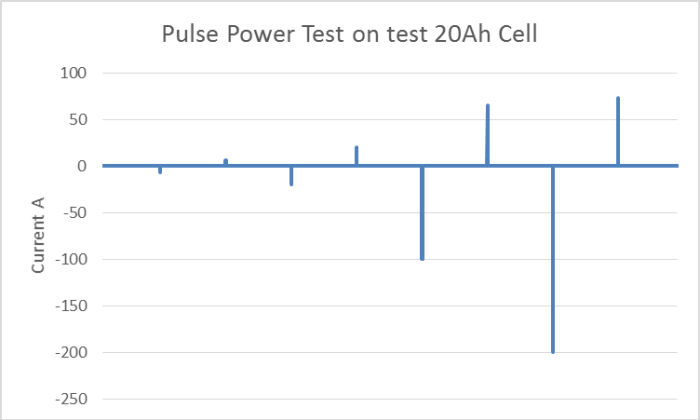

Figure 1: Pulse power test profile for a 20Ah test cell, charge profile is truncated for cell safety.

The researchers conducted the test exactly on the same 8 cells, using same battery test equipment. The cells were at the same SoC (50 %) and the tests were performed within a thermal chamber set to 25 °C. The battery test equipment used for this test has a current measurement accuracy of ±0.01 A and voltage measurement accuracy of ±0.001 V, the temperature sensors used to measure the temperature had an accuracy of ±0.5 °C. Following the experiment, areas to improve for reproducibility of the results across different researchers were identified.

2.2 Experiment 2 – improved experimental rig design to reduced number of connections

The test setup plays a vital role defining accuracy of the test results. To perform electrical characterisation tests, a set of current carrying cables are used to supply bidirectional current (charge/discharge) to the battery and another set of cables are used to sense the voltage. Ideally, the voltage sense cables should not be located within the current carrying path as this can result in errors due to voltage drops caused by any impedances within that path. However, the current amplitude used for electrical testing are increasing as battery power capability improve [9]. This requires multiple cycler channels to be connected electrically in parallel which in turn, means high numbers of cable connections are required. To reduce the complexity of experimental set-up a new approach was adopted whereby the voltage sense wire and current carrying conductor were crimped together in the same gold-plated lug. The gold plating reduced the connection resistance, thus the heat generation and protects the lug from corrosion, which avoids the need for cleaning before every time they are being used; justifying the additional cost.

Figure 2 (a) shows an example interconnection block, which is commonly used to connect battery cell tabs to the battery cycler cable. The block ideally should be large enough to connect the cycler cables and have large surface area to connect with cell tabs. However, it should be the smallest size possible to reduce unintentional cooling of the cell tab. The middle section of the lug is commonly used to connect the current carrying cables. For voltage sensors either top of the middle block or inner/outer post can be used, Figure 2 (b) shows an example of the voltage sensor connected on top of the current carrying cables. While such conditions are achievable, the setup time and physical space required for this configuration limits the quantity of testing that is able to be performed, and may create irregularities due to inconsistent setup and procedure.

A combined connection of voltage and current cables, just before connecting them to the interconnection block allows a more consistent setup as shown in Figure 2 (c). However, this places the voltage sense wire close to the current path. Therefore, an experiment was performed to investigate the effect of the location of the voltage sense cables on the experimental results. The test was performed on three 40 Ah NMC cells, which had an operating voltage window of 4.2 V – 2.7 V. The cells were charged-discharged with 0.5 C, 1C, 2 C and 3C current and the

tests were repeated for several location of the voltage sense cable with final test for the combined connections as shown in Figure 2 (c).

(a)

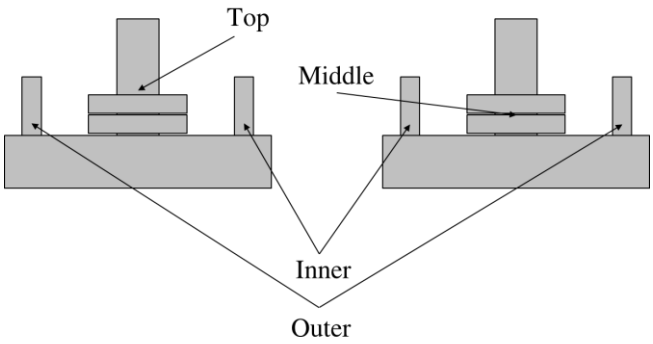

(b)

(c)

Figure 2: Interconnection between battery cell tabs and battery cycler, (a) design of the interconnection block (b) actual connection when voltage sensor connected on top (c) voltage sense cable crimped with current cable before connecting to interconnection block.

2.3 Experiment 3 – test chamber variation

Third experiment was conducted to investigate the effect of running the experiment in different thermal chambers to provide constant ambient temperature. For this experiment, same set of cells and test procedure as used in Experiment 1 were implemented, with the only exception that 80 % SoC was used. The test was undertaken in 4 different thermal chambers. The test was performed by the same researcher, using the same 8 cells and test rig. All the new knowledge learned from Experiment 1 and 2 to reduce experimental error, has been implemented in this experiment to keep the procedural errors to a minimum.

All the thermal chambers were set to 25 °C and the cells were allowed to soak at that temperature for a minimum of 4 hours. All these chambers use circulating air to maintain the temperature homogeneity across the volume. All of them are rated to maintain the test temperature within ±2 °C of the set temperature. Each thermal chamber is fitted with thermocouple(s) to monitor and maintain the set temperature, and all the chambers had valid calibration at the point of the experiment.

3. Results

3.1 Researcher variation

Internal resistance calculated from the PPT for all 8 cells and all 4 researchers are shown in Table 1. The standard deviation of the measurements from all eight cells (second row from the bottom), performed by any particular researcher include the cell to cell variation and the variation among the cell connections of that particular researcher. However, the standard deviation is still between 0.5 to 0.8 %, which indicates low cell to cell variation (environmental error) and good repeatability from each researcher. However, the variation among different researchers is around 4 % (environmental + procedural error). Therefore, while every researcher can reproduce their own setup it is not reproducible with high accuracy when different researcher performs the defined test-plan. This can be easily visualized from Figure 3, where internal resistance is plotted against maximum power discharged by the 10 C discharge pulse as part of PPT. As it can be seen, the results for all eight cells for each researcher are within close proximity but they shift for different researchers.

Table 1: Internal resistance calculated from all 8 cells

Cell	R 1 (mΩ)	R 2 (mΩ)	R 3 (mΩ)	R 4 (mΩ)	Mean (mΩ)	Standard Deviation	Std % of Mean
1	4.19	4.08	3.84	3.88	**4.00**	0.17	4.1%
2	4.17	4.08	3.82	3.86	**3.98**	0.17	4.3%
3	4.18	4.08	3.83	3.93	**4.01**	0.16	3.9%
4	4.15	4.05	3.81	3.85	**3.97**	0.16	4.1%
5	4.18	4.12	3.84	3.90	**4.01**	0.17	4.1%
6	4.12	4.03	3.79	3.91	**3.96**	0.14	3.6%
7	4.20	4.11	3.86	3.95	**4.03**	0.15	3.8%
8	4.16	4.08	3.83	3.88	**3.99**	0.16	4.0%
Mean	**4.17**	**4.08**	**3.83**	**3.89**	**3.99**	0.16	4.0%
Standard Deviation	0.02	0.03	0.02	0.03	0.02		
Std % of Mean	0.6%	0.7%	0.5%	0.8%	0.5%		

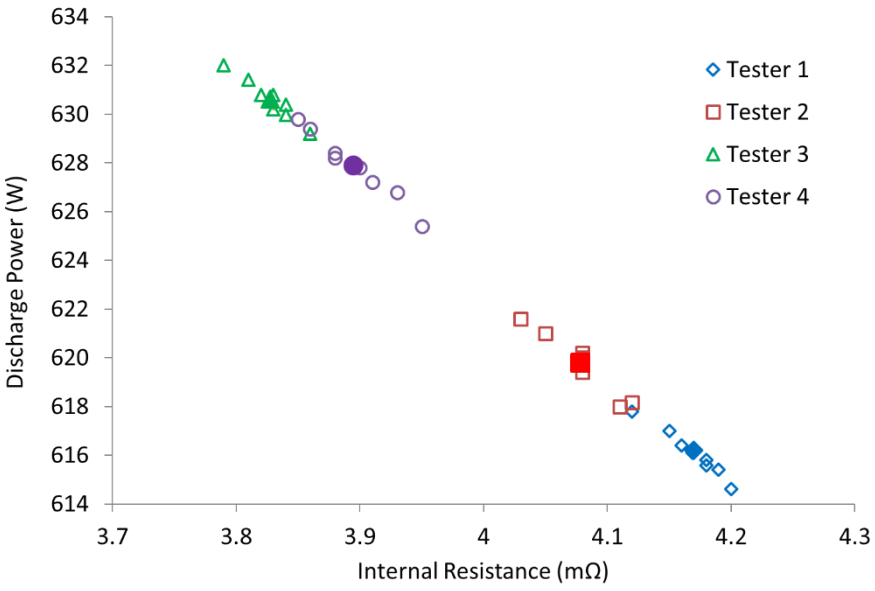

Figure 3: Discharge power versus internal resistance as carried out by 4 testers (**R**) on 8 test cells. Marker with the solid filling shows average value.

To find the root cause of the poor reproducibility, the test procedure has been investigated. All the researchers used the same battery test program, battery test equipment, connecting blocks of same design and test jig material. While no major deviations from the procedure were observed, it was noted that when connecting the battery cell tab and current carrying cables

from the battery cycler each researchers hand tightened the bolts used for the connections, which could lead to application of different torque, thus can be the source of the poor reproducibility. If different torque is applied, the quality of the interconnection between current carrying cables, connecting blocks and cell tabs will be different, leading to 10's to 100's μΩ contact resistance variations. Which may not be of large proportion of cell's internal resistance when cells have internal resistance of 10's to 100's mΩ (e.g. 18650, coin cells). However, when the cell resistance is much smaller, especially for high power/high energy cells (for the cells used here had around 4mΩ resistance), the variation will account for a relatively larger proportion of cell internal resistance. Another source could be the contact resistance variation due to oxidisation of the connectors, which required to be cleaned during the set-up process.

To investigate this hypothesis, the experiment was repeated with a modification. This time the researchers were provided with a calibrated torque wrench to ensure the cycler channel connection would always be connected with the same torque. To improve reproducibility of the connections, the connecting blocks were gold platted before the experiment was repeated. For the fixed torque, 12.5 Nm was employed, which was found to be optimal torque for the interconnection, any higher torque will not make significant reduction of the connection resistance.

The results show the procedure to be very reproducible (<1% error between experimenters), and the results can no longer be separated by researchers. This shows that the procedure has removed the key areas of variation identified. While an individual experimenter may produce repeatable results within their experiment, the omission of this information can have an impact on the reproducibility of results.

Table 2 shows the results from the repeated test. Cell to cell variation remained similar to that of earlier test. However, as expected, significant improvement has been observed for the researcher variation, compared to around 4% variation in earlier experiments (Table 1). As shown within Table is has reduced to around 0.4 %, where the researcher to researcher variation is now lower than the cell to cell variation. Figure 4 shows the pictorial representation of this improvement. Compared to Figure 3, a similar spread for cell-to cell variation has been

observed but in this case the results are concentrated into one particular area, making average values close to each other.

The results show the procedure to be very reproducible (<1% error between experimenters), and the results can no longer be separated by researchers. This shows that the procedure has removed the key areas of variation identified. While an individual experimenter may produce repeatable results within their experiment, the omission of this information can have an impact on the reproducibility of results.

Table 2: Internal resistance calculated from the repeated experiments with modification.

Cell	R 1 (mΩ)	R 2 (mΩ)	R 3 (mΩ)	R 4 (mΩ)	Mean (mΩ)	Standard Deviation	Std % of Mean
1	3.95	3.93	3.91	3.91	**3.92**	0.02	0.5%
2	3.88	3.91	3.90	3.89	**3.89**	0.02	0.4%
3	3.86	3.91	3.89	3.90	**3.89**	0.02	0.6%
4	3.89	3.90	3.87	3.88	**3.89**	0.01	0.3%
5	3.88	3.93	3.92	3.92	**3.91**	0.02	0.5%
6	3.89	3.87	3.88	3.87	**3.88**	0.01	0.3%
7	3.91	3.95	3.94	3.93	**3.93**	0.02	0.4%
8	3.91	3.91	3.88	3.87	**3.89**	0.02	0.5%
Mean	**3.90**	**3.91**	**3.90**	**3.90**	**3.90**	0.02	0.4%
Standard Deviation	0.03	0.02	0.02	0.02	0.02		
Std % of Mean	0.7%	0.6%	0.5%	0.6%	0.5%		

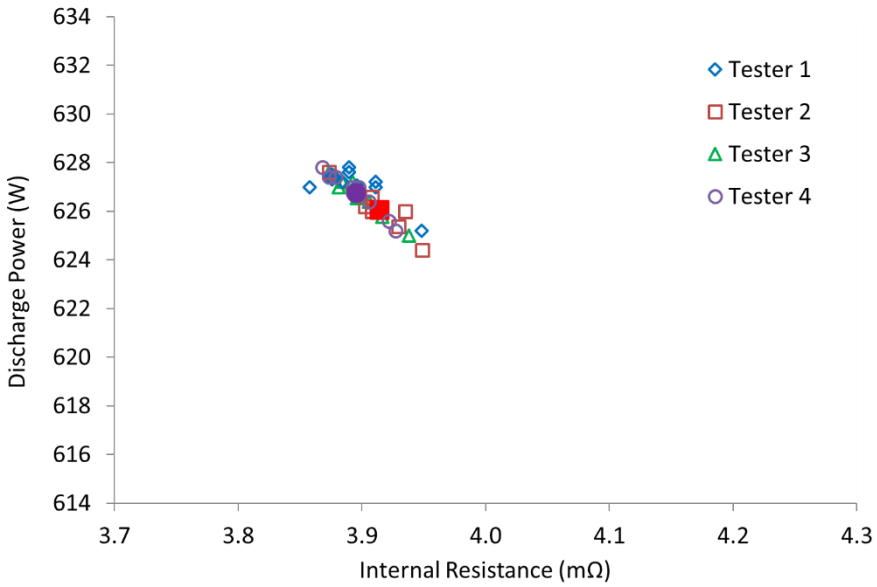

Figure 4: Discharge power versus internal resistance as carried out by 4 testers on 8 test cells after procedure was altered to include a torque wrench and gold platted connections. Marker with the solid filling shows average value.

3.2 Reduced cable connections and impact of voltage sensor location

Figure 5 shows the 1C discharge curves and voltage relaxation profiles recorded afterwards for different location of the voltage sensors. The longest discharge duration was achieved when the sensors were placed outside the connector and shortest duration when sensors was placed on the top, where the difference is 32.5 sec, e.g. 1% of average discharge duration. The variation between the ‘top’ and ‘middle’ location is 10.4 sec and 12.2 sec respectively between the outside and inside. This variation is because of the additional resistance on the current path.

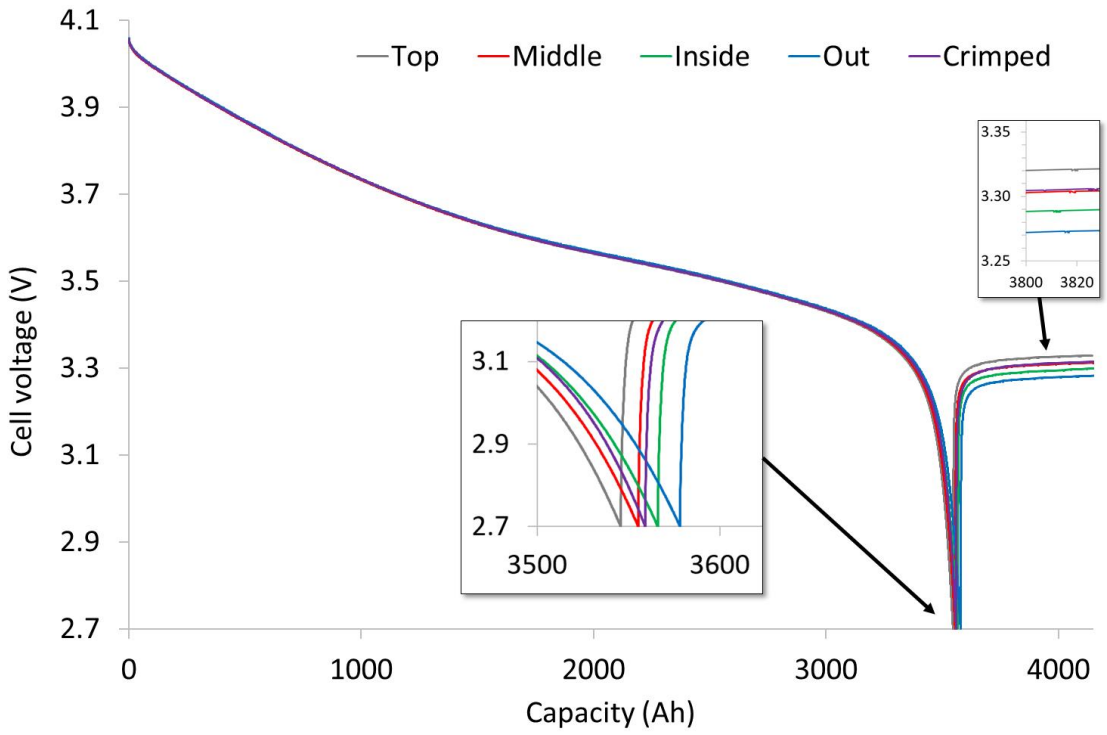

Figure 5: 1C discharge profile and voltage relaxation afterwards for different sensor locations.

The cell voltage is the open circuit voltage (OCV) minus the overpotential for the presence of the current ($V_{Cell} = V_{OCV} - I * R$). The resistance is the sum of the internal resistance of the cell and additional connector resistance between the cell to the location of the voltage sensor. Therefore, higher the resistance the faster it will reach to the discharge cut-off voltage of 2.7 V. When the voltage sense cable was placed on the top it included the longest current carrying path to the cell compared to any other location, therefore, it had the shortest discharge duration. Whereas the 'inner' and 'outer' locations were closest to the cell tab, away from current path, therefore, they had the longest discharge duration.

This hypothesis can be verified from the voltage relaxation history after the discharge. If the difference of the discharge duration is dominated by the resistance component variation ($I * R$) then for the 'top' location case cell had higher OCV when the cell voltage reached to 2.7 V and 'outer' location case OCV was lowest. The actual OCV of the cell was measured after the discharge ended and shown in Figure 5 with a zoomed view. The OCV for the 'top' location was 46 mV higher than the 'outer' location after the relaxation period, which is in line with the explanation earlier.

As mentioned earlier, the aim was to crimp the voltage sensor with the current carrying cable to improve repeatability and reproducibility of the connection. If by doing so introduces higher

degree of current path into the measurement, then it makes little sense to do so. However, from the results shown in Figure 5, when the sensor is crimped with the current carrying cable, it is actually on the middle, close to the average value. The discharge duration difference between 'crimped' case to the 'outer' case is 18.1 sec (0.5 %). Therefore, by placing the sensor closer to the cell, an improved result can still be achieved. However, with a sacrifice of 0.5 % accuracy a more repeatable and reproducible test setup can be achieved, which may led to higher confidence interval between results from multiple sets of experimentation.

The introduction of a new cable design and experimental rig has negatively impacted accuracy by 0.5%, however this has dramatically improved the repeatability and reproducibility of experimental test results with a seven-fold reduction in variation from 4.0% to 0.6% (Table 1 and 2). This has delivered a significant improvement in testing productivity by reducing the sample size required to achieve a predefined confidence value on the results acquired. For example, to achieve a 95% confidence on the test data a minimum of 12 sample size is required when the proposal made here are not implemented. However, with the implementation of the proposals made here only 3 samples are required to achieve such confidence level. This further helps to increase the numbers of experiments that can be performed on a given amount of equipment and reduce the costs of the experiments.

3.3 Chamber variations

The effect of chamber variation on test results are shown in Figure 6. The discharge power was higher compared to the results shown in Figure 3 and Figure 4, due to the fact the test was performed at a higher SoC. Although the same discharge current pulse applied, due to higher cell voltage at higher SoC, higher power was achieved. Compared to the cell to cell variation of 05-0.8 %, variation among the chambers were around 1.1 %. The variation may be related to how the chambers maintained the temperature and their respective capability to remove heat from the cell, which was generated during the pulse test. However, the variation is not significantly higher than the cell to cell variation, which can contribute to the results especially for long duration tests, where different chambers are used to test same battery performance. As mentioned, this type of environmental error cannot be reduced without making wholesale change to the facility, i.e. use chambers which can maintain temperature with a better accuracy, and require large capital investment.

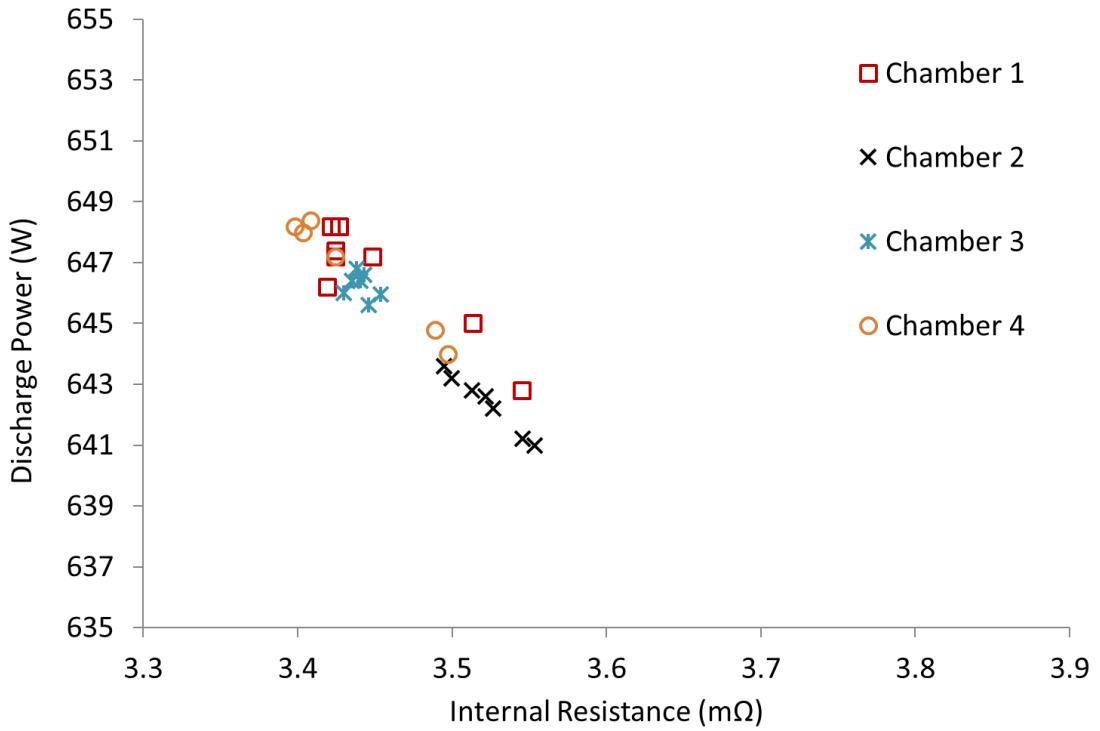

Figure 6: Discharge power versus internal resistance as carried out in 4 different chambers at 80 % SoC, 25 °C.

3.4 Other sources of error

In additional to these sources there are other sources which can introduce systematic errors (environmental error), one common one is battery tab material used for cylindrical cells. Compared to pouch and prismatic cells cylindrical cell tabs are at two sides and cell fixture like the ones shown in Figure 2 cannot be used. In such case, either a spring-loaded case is used to connect the cell to the test equipment or an additional tab is welded to the cell to allow use of fixture like the one in Figure 2. In first case, a variable error in introduced from the spring-loaded systems and in second case from tab material and welding quality. Tabs made of different tab materials such as copper, nickel, steel will have completely different resistance, therefore should be used uniformly within a test facility.

It has been shown in the previous sections, certain errors can be systematically accounted for, removed through better experimental design or shown to be a minor contributors, and there are other sources of error that cannot be removed e.g. cell-to-cell variation. Error reporting in the literature often is a result of experiments conducted, reporting the observed error from the results of the work [21]. The researcher accepts this error as the true result of their work, but

could be left concerned about the comparative uncertainty of their work. Without a guide to the amount of error to be expected from a result, the reported error is simply a statement of fact about the experiment as performed, and not a useful point of comparison in the amount of trust that can be placed in the uncertainty of the result.

4.0 Implementation of error into electrochemical modelling

To show an example of how the level of battery performance estimation accuracy can be improved by reducing experimental error from the dataset used for model parameterisation, a Pseudo Two Dimension model (P2D) has been parameterise using two sets of data having two different error values. The model is then employed to estimate battery performance degradation. The estimation from both cases is compared with the experimental data to calculate estimation accuracy.

Table 3 shows the list of electrochemical equations to capture the battery reaction kinetics using a P2D, solved over a porous layout [7]. The capacity fading or the degradation is captured by a continuous solvent reduction reaction presented in Ramadass et al. [22]. Measurement of battery performance and the degradation characteristics under different operating conditions are key in fine tuning the P2D based degradation model. A slight inaccuracy in measurement can cause erroneous estimation of solid electrolyte interphase (SEI) properties and side reaction intensity which makes the model unsuitable for EV or HEV warranty predictions. This section will analyse how an inaccurate measurement is carried over to subsequent predictions resulting in an uncontrolled error growth.

Fine tuning degradation characteristics based on experimentation is complicated since the property of the deposit (i.e. porosity, chemical composition etc.) can vary with different operating conditions. It has been observed that the side reaction characteristics and the SEI properties are different for cycling and storage. Therefore, to avoid complications and for increasing accuracy, parametrisation process is broadly divided into cycling capacity fade and storage capacity fade. In particular, for storage ageing parametrisation, the side reaction exchange current density, which is responsible for the intensity of degradation, is different for different SoC storage conditions. Therefore it is necessary to study a storage only or a cycling only condition for accurate parametrisation of an electrochemical model. The degradation model needs extensive chemical details of SEI, for example, thickness, density, molecular weight and conductivity. These parameters are very difficult to measure with the state of the

art technology [2]. Initial results of the parameterisation is given in Ashwin et al. [23], where the authors aimed to predict the SEI properties like density, molecular mass and conductivity by observing the trend of degradation for a storage only condition. Moreover, all other ageing mechanisms like dissociation, lithium plating etc. are lumped into SEI growth in most of the models.

In addition to SEI property estimation, there could be inaccuracies due to the basic cell characterisation. P2D models need more than twenty chemical parameters from each electrode. This uncertainty can influence the basic performance of the battery which will be carried over to degradation prediction. Electrochemical modellers are often faced with uncertainty and unavailability of chemical data during the parameterisation process and the model development. An accurate experimentation is expected to supplement additional data for model parameterisation thereby decreasing the modelling error. One common method to overcome this problem is to use literature values which is not recommended for blended electrodes [24]. Therefore, an OCV modification procedure is adapted and the electrochemical model has been parameterised using the available set of chemical parameters [23]. This model is found to be accurate up to ± 8mV over a drive cycle with acceleration and regenerative braking events. The most feasible option is to measure the performance characteristics accurately and fine tune the electrochemical model based on these learnings. The experimental methods, therefore, is the key in determining the accuracy since an erroneous electrochemical model can trigger erroneous controls in BMS, leading accelerated cell failures. The accuracy of the cell parameterisation strongly depends on voltage-current measurement which is improved by the methods described in previous sections.

All the electrochemical parameterisation studies for storage are conducted assuming that the measured degradation characteristics are the true values. The battery is stored at constant temperature of 25 °C and two different SoC values, 20% and 50%. Additional set of capacity characterisation tests were conducted after 1752, 3336, 4848 and 7128 hours of storage. This data will feed into the development of a correlation for solvent reduction side reaction. More details of this modelling methodology can be found in [2].

The experimental results and the model estimation for 20% SoC case is shown in Table 4. The capacity measurement at 1752 hours is taken as the parameterisation data for fine tuning the side reaction exchange current density (i_{os}) which will control the rate of degradation. Two models were developed for studying the impact of measurement error on subsequent modelling

prediction after 3336, 4848 and 7128hours. Model 1 is parameterised with a deviation of ± 0.07 % at 1752 hours of storage, which is amplified to ± 2.06 % after 3336 hours while the maximum deviation is found to be ± 4.42 % after 7128 hours. Model 2 was developed and parameterised by inducing a larger deviation of ± 0.72% compared to the experimentally measured data at 1752 hours. This error is amplified as ± 6.84 % after 7128 hours of storage. A similar observation can be made for 50% SoC storage as shown in Figure 6a, where the deviation of ± 2.26 % at 1752 hours is amplified to ± 8.86 % after 7128 hours of operation. Comparing the 20% and 50% SoC model predictions, the rate of error propagation is different for different SoC but it is similar for two different models at same SoC. This observation is made assuming that the property of SEI layer does not change with SoC.

These analysis shows that the measurement error in the parametrisation data propagates into the model prediction and will result in an inaccurate estimation of side reaction exchange current density. Moreover, the error can get amplified over a wide timespan in an electrochemical model.

Table 3: A summary of the governing equations for the electrochemical battery model

	Governing equations	***Boundary conditions***
Conservation of charge		
Electrolyte phase	$\nabla \cdot \left(\kappa_e^{eff} \nabla \phi_e\right) + \nabla \cdot \left[\kappa_{e,D}^{eff} \nabla \ln(c_e)\right] = -a_s(j+j_s)$	$\left.\frac{\partial \phi_e}{\partial x}\right\|_{x=0} = \left.\frac{\partial \phi_e}{\partial x}\right\|_{x=L} = 0$
Solid Phase	$\nabla . \left(\sigma_s^{eff} \nabla \phi_s\right) = a_s(j + j_s)$	$\left.\frac{\partial \phi_s}{\partial x}\right\|_{x=L^-} = \left.\frac{\partial \phi_s}{\partial x}\right\|_{x=L^+} = 0$ $-\sigma_{s,n}^{eff} \left.\frac{\partial \phi_s}{\partial x}\right\|_{x=0} = \frac{-I}{A}$ $= \sigma_{s,p}^{eff} \left.\frac{\partial \phi_s}{\partial x}\right\|_{x=L} = \frac{I}{A} = i(t)$
Conservation of lithium		
Electrolyte phase	$\frac{\partial(\varepsilon_e c_e)}{\partial t} = \nabla \cdot \left(D_e^{eff} \nabla c_e\right) + \frac{1 - t_+^0}{F} a_s(j + j_s)$	$\left.\frac{\partial c_e}{\partial x}\right\|_{x=0} = \left.\frac{\partial c_e}{\partial x}\right\|_{x=L} = 0$
Solid Phase	$\frac{\partial(\varepsilon_s c_s)}{\partial t} = \frac{D_s}{r^2} \frac{\partial}{\partial r}\left(r^2 \frac{\partial c_s}{\partial r}\right)$	$\left.\frac{\partial c_s}{\partial r}\right\|_{r=0} = 0, \left.\frac{\partial c_s}{\partial r}\right\|_{r=R_s} = \frac{-j}{a_s F}$
Kinetics		
Electrochemical reaction rate	$j = a_s i_0 \left\{exp\left[\frac{\alpha_a F}{RT} \eta_{n,p}\right] - exp\left[\frac{-\alpha_c F}{RT} \eta_{n,p}\right]\right\}$	
Exchange current density	$i_0 = F k_e (c_e)^{\alpha_a} (c_s^{max} - c_{s,e})^{\alpha_a} (c_{s,e})^{\alpha_c}$	
Solvent reduction reaction current density	$j_s = a_s i_{0s} e^{-\alpha_c f \eta_s}$	
Thickness of the SEI layer	$\frac{\partial \delta_{SEI}}{\partial t} = \frac{j_s M_p}{F \rho_p a_n}$	
Overpotential for the SEI reaction	$\eta_s = \phi_s - \phi_e - U_{ref} - j \frac{R_{SEI}}{a_s}$	
Overpotential for the negative electrode	$\eta_n = \phi_s - \phi_e - U - \frac{R_{SEI}}{a_s} j$	
Overpotential for the positive electrode	$\eta_p = \phi_s - \phi_e - U$	

Table 4: Capacity degradation results from calendar ageing test and the estimation by the electrochemical model.

Storage duration (hours)	20% SoC			50% SoC		
	Experimental value	Electrochemical model		Experimental value	Electrochemical model	
		Model 1	Model 2		Model 1	Model 2
0	3.05	3.05 (±0%)	3.05 (± 0%)	3.05	3.05 (± 0%)	3.05 (± 0%)
1752	2.99	2.99 (±0.07%)	2.97 (± 0.74 %)	3.01	2.95 (± 2.25%)	2.92 (± 3.25%)
3336	2.98	2.92 (±2.06%)	2.89 (± 3.06%)	3.01	2.86 (± 4.95%)	2.82 (± 6.28%)
4848	2.95	2.86 (±3.010%)	2.81 (± 4.71%)	2.96	2.79 (± 5.68%)	2.73 (± 7.71%)
7128	2.89	2.77 (±4.42%)	2.7 (± 6.84%)	2.93	2.68 (± 8.44%)	2.6 (± 11.17%)

5. Conclusion

Knowing the sources of error that can be introduced when testing batteries, the uncertainty in results can be quantified. In this manuscript it has been shown, that steps can be taken to ensure that random uncertainty can be reduced and isolated, and in some cases, a trade-off between error types can be made for repeatability and simplification of the experiments. Procedural errors cannot be quantified until the experiment has been done, so careful evaluation of process and test data is required after testing – repeated testing may be required to identify/improve the experimental design. It has been shown here that the level of procedural error can be reduced from more than 4 % to less than 1%. Environmental errors can be identified before running an experiment, here it was shown an environmental error of 1.1 % from cell-to-cell variation and chamber variation combined was expected.

In an extended testing environment, the knowledge of data quality is more important. When a large volumes of experimental data need to be assessed for their correctness quickly, and detailed analysis and consideration of their experimental error is time consuming to perform across all data. A pre-established error level defined during the design of the testing procedure gives the researcher the ability to judge the quality of the data after experimentation, before going through expensive and time-consuming processing.

Experiments will always produce errors, but by controlling the testing to ensure that only the baseline uncertainty happens, and that the testing procedure does not introduce additional errors, the quality of testing data can be ensured and give researchers confidence in going forward and reporting their findings. For the first time it was attempted to systematically quantify source of errors in battery testing and steps proposed to reduce the error levels. This shows how studying the uncertainties in battery testing methods can lead to improved outcomes of experimentation and provide researchers with greater confidence in the data being produced. This work will therefore, help the modelling community to predict battery performance with greater accuracy. The modellers will be also able to understand deeper about the inter-coupled chemical reactions, for which accurate measurements are a fundemtal requirement.

Acknowledgements

The research presented within this paper is jointly supported by the Innovate UK through the WMG centre High Value Manufacturing (HVM) Catapult in collaboration with Jaguar Land Rover and TATA Motors and EPSRC grant (EP/M009394/1).

References

1. Jaffe, S. *The battery industry: global marke sizing and forecast*. in *Benchmark Mineral Intelligence World Tour*. 2015. Toronto.
2. Ashwin, T.R., A. Barai, K. Uddin, L. Somerville, A. McGordon, and J. Marco, *Prediction of battery storage ageing and solid electrolyte interphase property estimation using an electrochemical model.* Journal of Power Sources, 2018. **385**: p. 141-147.
3. Uddin, K., S. Perera, W. Widanage, L. Somerville, and J. Marco, *Characterising Lithium-Ion Battery Degradation through the Identification and Tracking of Electrochemical Battery Model Parameters.* Batteries, 2016. **2**(2): p. 13.
4. Ye, Y., Y. Shi, N. Cai, J. Lee, and X. He, *Electro-thermal modeling and experimental validation for lithium ion battery.* Journal of Power Sources, 2012. **199**: p. 227-238.
5. Hu, X., S. Li, and H. Peng, *A comparative study of equivalent circuit models for Li-ion batteries.* Journal of Power Sources, 2012. **198**(0): p. 359-367.
6. Osaka, T., T. Momma, D. Mukoyama, and H. Nara, *Proposal of novel equivalent circuit for electrochemical impedance analysis of commercially available lithium ion battery.* Journal of Power Sources, 2012. **205**(0): p. 483-486.
7. Ashwin, T.R., Y.M. Chung, and J. Wang, *Capacity fade modelling of lithium-ion battery under cyclic loading conditions.* Journal of Power Sources, 2016. **328**: p. 586-598.
8. Schmalstieg, J., S. Käbitz, M. Ecker, and D.U. Sauer, *A holistic aging model for Li(NiMnCo)O2 based 18650 lithium-ion batteries.* Journal of Power Sources, 2014. **257**: p. 325-334.
9. Barai, A., K. Uddin, M. Dubarry, L. Somerville, A. McGordon, P. Jennings, and I. Bloom, *A comparison of methodologies for the non-invasive characterisation of commercial Li-ion cells.* Progress in Energy and Combustion Science, 2019. **72**: p. 1-31.

10. Ecker, M., J.B. Gerschler, J. Vogel, S. Käbitz, F. Hust, P. Dechent, and D.U. Sauer, *Development of a lifetime prediction model for lithium-ion batteries based on extended accelerated aging test data.* Journal of Power Sources, 2012. **215**(0): p. 248-257.
11. Wang, J., J. Purewal, P. Liu, J. Hicks-Garner, S. Soukazian, E. Sherman, A. Sorenson, L. Vu, H. Tataria, and M.W. Verbrugge, *Degradation of lithium ion batteries employing graphite negatives and nickel–cobalt–manganese oxide + spinel manganese oxide positives: Part 1, aging mechanisms and life estimation.* Journal of Power Sources, 2014. **269**: p. 937-948.
12. Schmidt, J.P., S. Arnold, A. Loges, D. Werner, T. Wetzel, and E. Ivers-Tiffée, *Measurement of the internal cell temperature via impedance: Evaluation and application of a new method.* Journal of Power Sources, 2013. **243**: p. 110-117.
13. Bloom, I., B.W. Cole, J.J. Sohn, S.A. Jones, E.G. Polzin, V.S. Battaglia, G.L. Henriksen, C. Motloch, R. Richardson, T. Unkelhaeuser, D. Ingersoll, and H.L. Case, *An accelerated calendar and cycle life study of Li-ion cells.* Journal of Power Sources, 2001. **101**(2): p. 238-247.
14. Barai, A., G.H. Chouchelamane, Y. Guo, A. McGordon, and P. Jennings, *A study on the impact of lithium-ion cell relaxation on electrochemical impedance spectroscopy.* Journal of Power Sources, 2015. **280**(0): p. 74-80.
15. Kindermann, F.M., A. Noel, S.V. Erhard, and A. Jossen, *Long-term equalization effects in Li-ion batteries due to local state of charge inhomogeneities and their impact on impedance measurements.* Electrochimica Acta, 2015. **185**: p. 107-116.
16. Spinner, N.S., C.T. Love, S.L. Rose-Pehrsson, and S.G. Tuttle, *Expanding the Operational Limits of the Single-Point Impedance Diagnostic for Internal Temperature Monitoring of Lithium-ion Batteries.* Electrochimica Acta, 2015. **174**: p. 488-493.
17. Widanage, W.D., A. Barai, G.H. Chouchelamane, K. Uddin, A. McGordon, J. Marco, and P. Jennings, *Design and use of multisine signals for Li-ion battery equivalent circuit modelling. Part 2: Model estimation.* Journal of Power Sources, 2016. **324**: p. 61-69.
18. Sautermeister, S., M. Falk, B. Bäker, F. Gauterin, and M. Vaillant, *Influence of Measurement and Prediction Uncertainties on Range Estimation for Electric Vehicles.* IEEE Transactions on Intelligent Transportation Systems, 2018. **19**(8): p. 2615-2626.
19. 62660-1, I., *Secondary lithium-ion cells for the propulsion of electric road vehicles – Part 1: Performance testing*. 2012, International Electrotechnical Commission: Geneva, Switzerland.
20. Barai, A., K. Uddin, W.D. Widanage, A. McGordon, and P. Jennings, *A study of the influence of measurement timescale on internal resistance characterisation methodologies for lithium-ion cells.* Scientific Reports, 2018. **8**(1).
21. Beelen, H.P.G.J., L.H.J. Raijmakers, M.C.F. Donkers, P.H.L. Notten, and H.J. Bergveld, *A comparison and accuracy analysis of impedance-based temperature estimation methods for Li-ion batteries.* Applied Energy, 2016. **175**: p. 128-140.
22. Ramadass, P., B. Haran, P.M. Gomadam, R. White, and B.N. Popov, *Development of First Principles Capacity Fade Model for Li-Ion Cells.* Journal of The Electrochemical Society, 2004. **151**(2): p. A196-A203.
23. Ashwin, T.R., A. McGordon, W.D. Widanage, and P.A. Jennings, *Modified electrochemical parameter estimation of NCR18650BD battery using implicit finite volume method.* Journal of Power Sources, 2017. **341**: p. 387-395.
24. Chikkannanavar, S.B., D.M. Bernardi, and L. Liu, *A review of blended cathode materials for use in Li-ion batteries.* Journal of Power Sources, 2014. **248**: p. 91-100.